

VDI

Entwicklung
Konstruktion Vertrieb

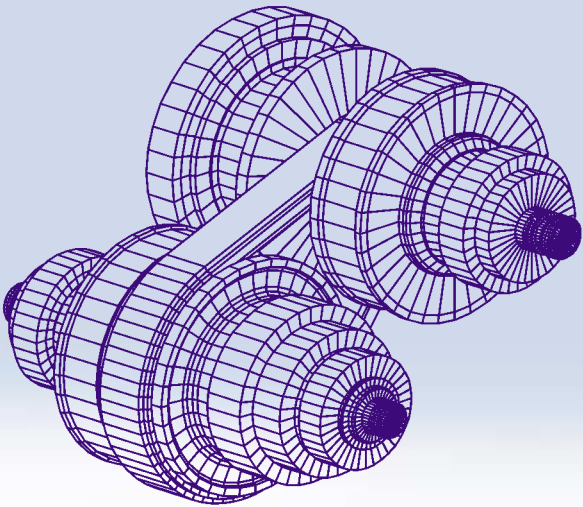
Programme

October 7th/8th, 2002

in Munich/Germany, Forum Hotel

with exhibition

CVT 2002 Congress



TWO-DIMENSIONAL VISCOELASTICITY IN RUBBER V-BELT DRIVES

Prof. Francesco Sorge and Dr. Marco Cammalleri

Department of Mechanics and Aeronautics, University of Palermo

Viale delle Scienze, 90128 - Palermo, Italy

Phone: +39 091 6657157-6657160, Fax: +39 091 6657163

E-mail: <sorge@dima.unipa.it>, <cammalleri@dima.unipa.it>

ABSTRACT

The viscoelastic response of rubber V-belts is treated by a three-parameter constitutive model, where a spring is added in parallel to the Maxwell element. The viscoelasticity is considered in both the longitudinal and transverse deformation. In particular, the study aims at improving the wear resistance and the durability of the belt taking advantage of the slip decrease along the pulley due to the viscous retard in the deformation. An extensive experimentation has been carried out on some commercial belts, detecting the long-time viscoelastic properties and permitting a rough evaluation of the constitutive parameters to be used in a drive. The mathematical model for the viscous belt drive is solved numerically by Runge-Kutta routines and square error minimisation techniques through a steepest descent procedure. This permits quantifying the belt slip reduction, which is negligible for actual belts, but could be significantly enhanced by a proper selection of the belt materials.

1. INTRODUCTION

A rubber belt must be considered as a composite mechanical component, where the internal cord is subject to the longitudinal tension and the rubber body transmits the torque to the pulley walls. Interesting results can be obtained by modifying the viscoelastic properties of the belt materials. For example, an increase of the internal cord viscoelasticity might be advantageous for the wear resistance, because the belt slip would be reduced [1, 2].

The stress-strain behaviour of polymers can be modelled by combinations of Kelvin-Voigt elements (spring and dashpot in parallel) and Maxwell elements (spring and dashpot in series). The greater is the number of elements, the finer is the accuracy. The application of the three-parameter model (Maxwell element plus a shunt spring) to the main directions of the belt yields the following constitutive relationships [3]:

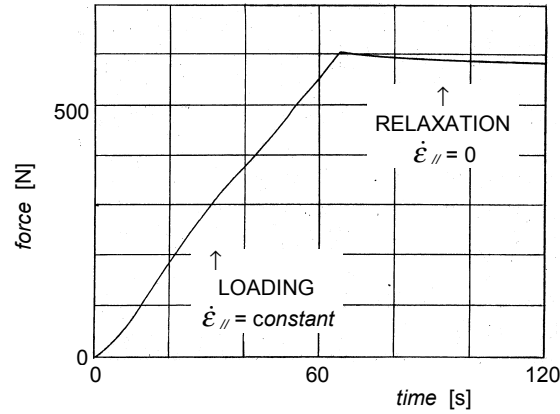


Figure 1. Load-relaxation test on a piece of belt
(cogged V-belt, wedge angle = 14°, width = 15 mm, thickness = 4 mm + cogs)

$$T + \tau_{R//} \dot{T} = S_{//} (\epsilon_{//} + \tau_{C//} \dot{\epsilon}_{//}) \quad (1.1)$$

$$\sigma_c + \tau_{R\perp} \dot{\sigma}_c = E_{\perp} (\epsilon_{\perp} + \tau_{C\perp} \dot{\epsilon}_{\perp}) \quad (1.2)$$

where the dots mean derivatives with respect to the time, the subscripts $(.)_{//}$ and $(.)_{\perp}$ refer to the directions parallel and normal to the belt axis, T is the tension force, σ_c is the transverse compression stress, $\epsilon_{//}$ and ϵ_{\perp} are the longitudinal elongation and the transverse compression strain. Equations (1.1) and (1.2) contain the constitutive parameters of the belt: $S_{//}$ and E_{\perp} give the longitudinal stiffness of the whole belt and the rubber elastic modulus at the elastic equilibrium, $\tau_{R//}$ and $\tau_{R\perp}$ are viscous relaxation times, $\tau_{C//}$ and $\tau_{C\perp}$ are viscous creep times, dependent on the temperature and on the duration of the phenomenon to be considered. Power belt drives imply deformation times of the order 10^{-2} s, while the static loading on a tension testing machine is much slower (Fig. 1). Very different values of the viscous retardation times are to be expected for the two cases.

2. EXPERIMENTS

Several experimental tests were carried out to detect the belt properties. Some commercial V-belts with similar characteristics were wound on two cast-iron pulleys and loaded by a tension-testing machine. Other tests were carried out overturning and winding the V-belts on two nylon band pulleys for a flat belt simulation. The pulley centre distance was increased in all the tests at the constant speed of 2.5 mm/min and then decreased. A remarkable hysteresis effect was observed due to the pulley

friction. Moreover, V-belts gave rise to much higher displacements than flat belts owing to the wedging into the groove, equivalent to a compliance increase.

The friction coefficient $f = \tan\phi$ was calculated separately by dynamometric tests and the following results were obtained: $f \cong 0.3$ (pulley wall - belt side), $f \cong 0.12$ (nylon pulley - belt back).

The theoretical analysis of the load tests is reported in Refs. [2, 4], giving the interpretation of the experimental plots. The length increase $s - s_0$ of a piece of belt starting from the middle plane of symmetry through the pulley axes is calculated in dependence on the radial penetration on the one hand, on the elongation $\varepsilon_{//}$ on the other hand and the two expressions are equated. Such a "mass conservation" condition is associated with the equilibrium equations, normal and parallel to the belt, completing the analytical definition of the problem.

Significant quantities appear in this analysis and will be also used in the following. The stiffness parameter $k = 2 \tan\alpha S_{\perp} / S_{//}$ compares the transverse and longitudinal rigidities of the belt [5]. The transverse bending ratio $B = \varepsilon_w / \varepsilon_{//} > 1$ accounts for the radial deflection of the belt cross-section, which involves a decrease of the longitudinal elongation from the sides toward the mid-plane and then a lower value of the mean elongation $\varepsilon_{//}$ with respect to the wall value ε_w [6]. The sliding angle γ is formed by the resultant friction force in the plane of rotation and the radius, while the angle $\beta = \arctan [f \tan\gamma / (f \pm \sin\alpha \sqrt{1 + \tan^2\gamma + \tan^2\alpha})] = \beta(\tan\gamma)$ is formed by the resultant wall force, where the double sign refers to $\cos\gamma > 0 (+)$ or $\cos\gamma < 0 (-)$.

A third order differential system has to be solved for the three unknowns $\varepsilon_{//}$, x and γ in dependence on the angular coordinate θ . Assuming for simplicity the "isotropic" hypothesis of equal retardation times in the longitudinal and transverse directions, i. e. $\tau_{R//} = \tau_{R\perp}$ and $\tau_{C//} = \tau_{C\perp}$, one gets uncoupling between the space and time domains and may assume distributions of the separable variable type for the unknowns. Moreover, the sliding angle γ is found to depend only on θ , i. e. the belt elements penetrate along logarithmic spirals.

The solution can be obtained in closed form and, adjusting the physical parameters of the belt by tentative in order to get a good fit with the experimental diagrams, comparing the results for V- and flat belts, the following numbers were roughly estimated: $\tau_{R//} \cong 27$ s, $\tau_{C//} \cong 40$ s, $k \cong 0.15$. The other belt characteristics were: $\alpha = 14^\circ$, $B \cong 2.5$.

3. TWO-DIMENSIONAL ANALYSIS OF V-BELT DRIVES

3.1. Scheme of a viscous V-belt drive

Let us assume a V-belt drive in steady operation and consider the material response from the Eulerian point of view. Along the winding arc over the pulley, it is more convenient to use the unit angle axial force Z and the dimensionless radial penetration $x = -\Delta r/r_0$ in place of σ_c and ε_{\perp} , where r is the radius and the subscript $(\cdot)_0$ refers to zero load. However, the variable x is proportional to ε_{\perp} : $x = \varepsilon_{\perp} H/r_0$, where H is the groove depth.

Introducing the transverse stiffness of the belt $S_{\perp} = hE_{\perp}r_0^2 / H$, where h is the equivalent belt thickness, and the dimensionless forces $t = T / S_{\parallel}$ and $z = Z / S_{\perp}$, one may change the constitutive equations, Eqs. (1.1) and (1.2), into the following form:

$$t + \frac{\omega\tau_{R\parallel}t'}{1 - \tan\chi \tan\gamma} = \varepsilon_{\parallel} + \frac{\omega\tau_{C\parallel}\varepsilon'_{\parallel}}{1 - \tan\chi \tan\gamma} \quad (\text{along the arc of contact}) \quad (3.1)$$

$$\varepsilon_{\parallel} + v\tau_{C\parallel} \frac{d\varepsilon_{\parallel}}{ds} = t \quad (\text{along the free span}) \quad (3.2)$$

$$\left(\frac{z \cos\chi}{1-x} \right) + \frac{\omega\tau_{R\perp}}{1 - \tan\chi \tan\gamma} \left(\frac{z \cos\chi}{1-x} \right)' = x + \frac{\omega\tau_{C\perp}x'}{1 - \tan\chi \tan\gamma} \quad (\text{along the arc of contact}) \quad (3.3)$$

$$\varepsilon_{\perp} + v\tau_{C\perp} \frac{d\varepsilon_{\perp}}{ds} = 0 \quad (\text{along the free span}) \quad (3.4)$$

where primes indicate derivatives with respect to the angular coordinate θ along the arc of contact, ω and v are the angular velocity of the pulley and the belt velocity and χ is the penetration angle, formed by the belt trajectory and the circumferential direction. The factor $\cos\chi / (1-x)$ is justified in Eq. (3.3) by the relationship $ds = r d\theta / \cos\chi = r_0 (1-x) d\theta / \cos\chi$ between the length ds of a belt element and the variation $d\theta$. The denominator $1 - \tan\chi \tan\gamma$ appearing in Eqs. (3.1) and (3.3) can be easily understood considering Eq. (3.8) below.

The constancy of the belt tension and the vanishing of the transverse compression stress along the free span justify equations (3.2) and (3.4), because no external force is applied there, but the creep is still progressing.

The approximate approach of Refs. [1, 2] applies quite well to the mechanics of viscous V-belts, but accounting for the two-dimensional viscoelasticity. The belt path is divided in several parts like in Fig. 2 and the belt-pulley interaction is studied according with usual models [5, 7]. Each region is solved separately starting from its own initial point and then the solutions are connected to each other, fulfilling the variable continuity and obtaining a piece-wise global solution.

Considering an elastic belt, the belt-pulley coupling presents three degrees of freedom: the extension of the wrap arc and the forces on the entrance and exit side. This agrees with three

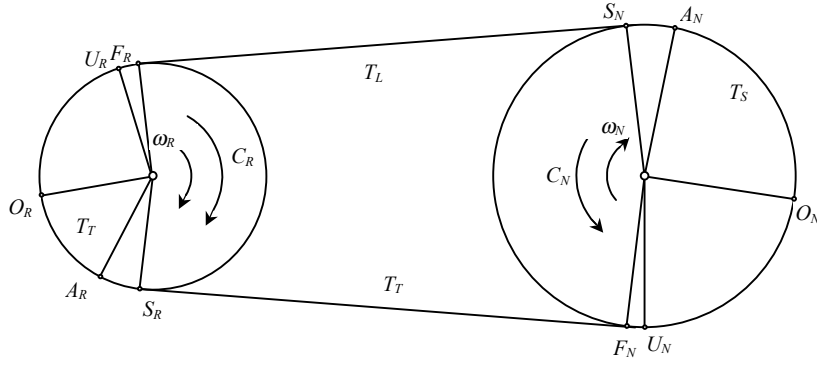


Figure 2. Scheme of the various regions along the belt path

Subscripts: (...) _R = driver pulley, (...) _N = driven pulley, (...) _T = tight span, (...) _L = loose span
 SA = seating region, AO = adhesion-like region, OU = main sliding region, UF = unseating region

constraints to be imposed, pre-forcing, torque and winding width. When dealing with a viscoelastic belt, we have two extra variables ($t \neq \varepsilon_{//}$, $z \neq x(1-x)/\cos\chi$) and two extra differential equations (the constitutive equations above), that is five degrees of freedom in total, and must then impose also the circular continuity of the variables along the closed belt path.

3.2. Main sliding arc

A fifth order differential system and a finite equation are to be written, in the six variables t , $\varepsilon_{//}$, z , x , χ and γ , i. e. Eqs. (3.1), (3.3) and:

$$t' = t(1 + \chi') \tan(\beta + \chi) \quad (\text{equilibrium // belt}) \quad (3.5)$$

$$t(1 + \chi') = kz \cos \chi \left(\frac{1 - \tan \beta \tan \chi}{\tan \beta} \right) \quad (\text{equilibrium } \perp \text{ belt}) \quad (3.6)$$

$$x' = (1 - x) \tan \chi \quad (\text{geometry}) \quad (3.7)$$

$$1 - \tan \chi \tan \gamma = \frac{\omega r}{v \cos \chi} = \frac{(1 + B\varepsilon_{//O})(1 - x) \cos \chi_O}{(1 + B\varepsilon_{//})(1 - x_O) \cos \chi} \left(\frac{\omega r_O}{v_O \cos \chi_O} \right) \quad (\text{kinematics + mass conservation}) \quad (3.8)$$

where the subscript (\cdot)_O indicates a reference point O somewhere along the belt path.

The solution depends on six constants for each pulley, $\varepsilon_{//O}$, x_O , χ_O , γ_O , z_O and t_O , in accordance with the number of degrees of freedom above (as the position of point O is arbitrary, the arc of contact Θ splits in two parts, $\Theta_{upstream}$ and $\Theta_{downstream}$, involving thus a sixth "degree of freedom").

Neglecting small terms, the previous equations, Eqs. (3.1), (3.3) and (3.5) to (3.8), can be abridged to the form:

$$t' = t \tan \beta \quad (3.9)$$

$$t = kzF(\gamma) \quad \text{where } F(\gamma) = \left(1 - \frac{\tan \beta}{\cos^2 \alpha \tan \gamma} \right)^{-1} \quad (3.10)$$

$$x' \tan \gamma = x - x_0 + B(\varepsilon_{//} - \varepsilon_{//0}) + s_0 \quad \text{where } s_0 = x'_0 \tan \gamma_0 \quad (3.11)$$

$$t + \omega \tau_{R//} t' = \varepsilon_{//} + \omega \tau_{C//} \varepsilon'_{//} \quad (3.12)$$

$$z + \omega \tau_{R\perp} z' = x + \omega \tau_{C\perp} x' \quad (3.13)$$

It is interesting that the belt inertia can be considered as well in the present analysis by simply giving to t and $\varepsilon_{//}$ the meaning of dynamic force and elongation, $t - qv^2/S_{//}$ and $\varepsilon_{//} - qv^2/S_{//}$, where qv^2 is the momentum flux.

Equation (3.10) can be solved for $\tan \gamma$

$$\tan \gamma = \pm \frac{\sqrt{(1 - f^2 \tan^2 \alpha)(k_1 z - t)(t - k_2 z)}}{\cos \alpha (t - kz)} \quad (3.14)$$

where $k_1 = k \tan(\alpha + \varphi) / \tan \alpha$, $k_2 = k \tan(\alpha - \varphi) / \tan \alpha$ and the double sign refers to the driven (+) and driver pulley (-) respectively [5].

Then, since $t \tan \beta = (t - kz) \cos^2 \alpha \tan \gamma$ by Eq. (3.10), Eqs. (3.9) to (3.13) contract to a fourth order differential system for the unknowns t , z , x and ε :

$$t' = \pm \cos \alpha \sqrt{(1 - f^2 \tan^2 \alpha)(k_1 z - t)(t - k_2 z)} \quad (3.15)$$

$$x' = \pm \cos \alpha \frac{(x - x_0 + B\varepsilon_{//} - B\varepsilon_{//0} + s_0)(t - kz)}{\sqrt{(1 - f^2 \tan^2 \alpha)(k_1 z - t)(t - k_2 z)}} \quad (3.16)$$

$$\varepsilon'_{//} = \frac{t - \varepsilon_{//} \pm \omega \tau_{R//} \cos \alpha \sqrt{(1 - f^2 \tan^2 \alpha)(k_1 z - t)(t - k_2 z)}}{\omega \tau_{C//}} \quad (3.17)$$

$$z' = \frac{x - z \pm \omega \tau_{C\perp} \cos \alpha \frac{(t - kz)(x - x_O + B\varepsilon_{//} - B\varepsilon_{//O} + s_O)}{\sqrt{(1 - f^2 \cos^2 \alpha)(k_1 z - t)(t - k_2 z)}}}{\omega \tau_{R\perp}} \quad (3.18)$$

3.3. Adhesion-like region. Free span. Reference point O

In accordance with recent theoretical findings [8] and with numerical results from the previous full differential system, the adhesion-like concept has to be introduced in the analysis in place of the idle arc. The belt tension does not vary appreciably along the adhesion-like region and the creep proceeds from the straight span through the seating region inside the arc of contact.

Since the belt tension is nearly constant also along the boundary regions and moreover, it is necessarily constant along the free span due to the absence of external forces on the belt surface, a unique solution is valid along the whole tract $U_{N,R} O_{R,N}$ (Fig. 2):

$$t = \text{constant} = t_{TL} \quad (3.19)$$

$$\varepsilon_{//} = t_{TL} + (\varepsilon_{//U} - t_{TL}) \exp[(s_U - s) / v \tau_{C//}] \quad (3.20)$$

The transverse variables x and z will be obtained in the adhesion-like region by prolonging the seating solutions, which will be derived in the following subsection. As regards the free span, Eq. (3.4) gives

$$z = 0 \quad (3.21)$$

$$\varepsilon_{\perp} = \varepsilon_{\perp F} \exp[(s_F - s) / v \tau_{C\perp}] \quad \varepsilon_{\perp F} = x_F \frac{r_{0F}}{H} \quad \varepsilon_{\perp S} = \varepsilon_{\perp F} \exp(-l_{free\ span} / v \tau_{C\perp}) = x_S \frac{r_{0S}}{H} \quad (3.22)$$

Notice that $z = 0$ but $x \neq 0$ at points F and S , as the viscoelastic strain is not in phase with the stress.

The diagrams of the two quantities t and $\varepsilon_{//}$ must necessarily intersect twice along the belt path and in particular, they do it inside the sliding arcs of the driver and driven pulley. In fact, the variable periodicity implies the vanishing of the integral $\oint (\tau_{C//} d\varepsilon_{//} / ds - \tau_{R//} dt / ds) v ds$, which is equal in turn to $\oint (t - \varepsilon_{//}) ds$ and could not vanish for $t \neq \varepsilon_{//}$ everywhere. Since no intersection is possible where t is constant (or nearly constant) in contrast with the constitutive equations, the two points of intersection lie in the sliding arcs. As the experiments indicate that $\tau_{C//} > \tau_{R//}$, the slope of the $\varepsilon_{//}$ curve is lower than

t at these intersections and thus, the starting value of $\varepsilon_{//}$ in the sliding region is a little lower than t on the driver pulley and a little higher on the driven pulley.

Suppose to fix the reference point O , i. e. the initial point of the main sliding arc, at that particular position where $\varepsilon_{//}$ becomes stationary, i. e. maximum in the driver pulley and minimum in the driven pulley, before starting its rapid variation. The numerical results indicate that this condition corresponds to $x'' \cong 0$ roughly for the driven pulley and to $x' \cong 0$ for the driver pulley. Moreover, the variables z and x are nearly equal there.

Therefore, putting $\varepsilon_{//}' = 0$, Equation (3.17) gives z_O in dependence on t_O and $\varepsilon_{//O}$. Between the two roots of this quadratic equation, the one closer to the value t / k_1 is to be chosen (nearly stationary t). Then, it is possible to calculate s_{ON} for the driven pulley by differentiating Eq. (3.16) with respect to θ and putting $x''_{ON} = 0$, while s_{OR} is simply equated to zero for the driver pulley.

3.4. Seating and unseating

Inside the two short regions at the entrance and the exit of the wrap arc, the penetration gradient becomes relatively large. Equation (3.6) shows that $\chi' = -1$ at the ends of the wrap arc, where $z = 0$, and thus the gradient of χ is not negligible inside the boundary regions, differently from the main sliding arc. Furthermore, Eq. (3.8) shows that $\tan\gamma$ becomes small in these regions, because of the increase of $|\chi|$. In practice, we are in front of a problem of the boundary layer type and a different approximate formulation must be used with respect to Section 3.2 [6].

Assuming $\gamma \cong 0^\circ$ in the seating region (where the belt penetrates) and $\gamma \cong 180^\circ$ in the unseating region (where the belt emerges), the tension t is nearly constant there ($\tan\beta \cong 0$). Thus, considering the new order of magnitude of the variables, Equations (3.6) and (3.7) reduce to

$$x'' - \frac{\kappa z}{t} = -1 \quad \text{where } \kappa = k_1 \text{ in the seating region and } \kappa = k_2 \text{ in the unseating region} \quad (3.23)$$

The viscoelastic equation still holds in the form (3.13).

Multiplying Eq. (3.13) by κ / t , summing Eq. (3.23) and observing that $\kappa z' / t = x'''$ by Eq. (3.23), the following third order differential equation is obtained for the boundary regions:

$$x''' + \frac{1}{\omega\tau_{R\perp}} x'' - \frac{\kappa\tau_{C\perp}}{t\tau_{R\perp}} x' - \frac{\kappa}{t\omega\tau_{R\perp}} x = -\frac{1}{\omega\tau_{R\perp}} \quad (3.24)$$

where the unitary axial force is given by $z = (1 + x'') t / \kappa$.

Five conditions are imposed: zero axial force at the outer end and matching of the radial penetration, of the axial force and of their gradients with the inner solution at the inner end. Nevertheless, they are in practice four, because one is redundant due to Eq. (3.13). Four are also the constants to be determined, the three integration constants of Eq. (3.24) and the unknown angular width of the boundary region.

Once the solution is obtained, the outer end radial penetration can be calculated. As was previously said, such a non-zero value must not surprise, since the deformation does not vanish simultaneously with the force for a viscoelastic material. The transverse deformation goes on creeping along the free span, according to Eq. (3.22), and matching with the downstream outer value of the other pulley, at the end of the straight strand.

Using realistic values for the constitutive parameters of the belt, the three characteristic roots ρ_i of the cubic equation associated with Eq. (3.24) are generally real for the seating region and in particular, one is positive (say ρ_1) and the other two are negative (ρ_2 and ρ_3). On the contrary, a pair of complex roots is found in the unseating region, unless the friction coefficient f is very small, in which case all the roots are real.

Indicating with δ the angular distance from the outer end ($\delta = \theta - \theta_{in}$ or $\theta - \theta_{out}$ for the seating or unseating region), the solution can be written in the form:

$$x = \frac{t}{\kappa} \left[1 + \sum_1^3 c_i \exp(\rho_i \delta) \right] \quad z = \frac{t}{\kappa} \left\{ 1 + \frac{t}{\kappa} \left[\sum_1^3 c_i \rho_i^2 \exp(\rho_i \delta) \right] \right\} \quad (3.25)$$

Imposing the boundary conditions, four linear algebraic equations arise, in the three unknown constants c_i . The fourth unknown δ_{inner} , angular width of the boundary region, appears in the exponential factors and can be found by imposing the linear inter-dependence of the system equations, i. e. equal rank (three) of the system matrix and of the augmented matrix. This transcendental condition can be solved by iterative procedures.

Since the idle-like condition, $z'_{inner} \cong 0$, $z_{inner} \cong t/\kappa = t/k_1$, $x'_{inner} \cong 0$, $x_{inner} \cong t/\kappa = t/k_1$, can be applied at the inner end of the seating arc, the coefficient c_1 must be equated to zero in Eqs. (3.25). This involves that the angular extent of the seating region is somewhat larger than the unseating one, similarly to the elastic case [6, 8]. At the exit side on the contrary, the connection between the main sliding and unseating arcs takes place with approximately constant penetration and tension, but with a very sharp change of the sliding angle, as is clearly visible by the numerical results from the full system.

Observe also that, differentiating Eqs. (3.25) for $\delta = 0$, the entrance and exit angles of the belt can be obtained and the torque can be calculated in dependence on these angles, on the local radii ($\neq r_0$) and on the belt forces in the tight and slack sides. This is useful for the evaluation of the efficiency losses of a thin belt due to the boundary friction.

Other effects influence the efficiency of a V-belt drive, e. g. the angular speed slippage because of the different elongation and penetration along the adhesion-like regions on the driver and driven pulleys, the bending hysteresis loss due to the cyclic seating and unseating of the belt on the pulley, the losses at the pulley bearings, or because of the air drag during the rotation, etc.

4. NUMERICAL APPROACH

The mathematical problem described so far is substantially non-linear and moreover, is defined over a fragmentary domain with unknown internal boundaries among the various parts. Fixing the geometry of the drive, the physical characteristics of the belt and the tension in the tight and slack sides, three quantities are to be determined for each pulley: the extent of the main sliding arc, the extent of the unseating arc and the starting elongation of the main sliding region. Four of these unknowns will be searched numerically by a square error minimisation process applied to the discontinuities among the various parts of the piece-wise solution, while the widths of the unseating regions will be simply updated at each iteration using the latest values of x_{inner} , x'_{inner} , z_{inner} and z'_{inner} for the calculation of the solutions (3.25). As regards on the contrary the seating solutions, they will match asymptotically and automatically to the adhesion-like solutions during the numerical calculation.

For each pulley in practice, some starting values are imposed to the widths of the sliding and unseating arc and to the initial sliding elongation, and z_0 , x_0 and s_0 are calculated as was described in the last paragraph of Section 3.3. Then, Eqs. (3.15) to (3.18) are solved by a fourth order Runge-Kutta routine as far as the end of the sliding arc and Eqs. (3.19) to (3.22) are used to prolong the solution to the end of the adhesion-like region of the other pulley downstream. At this point, the tension and elongation are compared with the starting values used for the other pulley and the sum of the square errors is used as a criterion function to be minimised.

The minimisation process follows the steepest descent technique, where the gradient of the criterion function is calculated numerically by changing one variable at a time. Then, the search moves "downhill" along the gradient direction making use of a dichotomous procedure, i. e. by halving the step size successively until a minimum of the criterion is achieved. At this local minimum, a new gradient vector is computed and then the search goes on in the same way as far as the final convergence is attained (criterion function $< 10^{-6}$) [9].

In order to avoid numerical instability, the minimisation is carried out only for the two angular widths of the sliding arcs during a first phase of the calculation and the starting elongation is equated to the tension variable t_o . This implies the vanishing of t'_o , γ_o and s_o by Eqs. (3.17), (3.15), (3.14) and (3.11) and involves the tension-compression relationship $t_o = k_1 z_o$. The penetration gradient x'_o vanishes as well and thus, point O is recognised as an orthogonal point in the sense of Lutz [10]. Proceeding as in [5] but taking into consideration also the viscous relationships, the trajectory directions at such a singular point in the four-dimensional space of the sliding solutions are given by

$$\frac{dt}{dx} = u_{\pm} \quad \frac{d\varepsilon_{//}}{dt} = \frac{\tau_{R//}}{\tau_{C//}} \quad \frac{dx}{dz} = \frac{\tau_{R\perp}}{\tau_{C\perp}} \quad (4.1)$$

where the symbol u_{\pm} indicates the two roots of the quadratic equation

$$u^2 + u(3 - 2f \tan \alpha) \frac{\tau_{C//}}{B\tau_{R//}} - 2k \left(1 + \frac{f}{\tan \alpha}\right) \frac{\tau_{C//}\tau_{C\perp}}{B\tau_{R//}\tau_{R\perp}} = 0 \quad (4.2)$$

and the double sign refers to the driven (+) and driven pulley (−) respectively.

Point O is a saddle-like singularity and the two separatrices springing from O are the images of the driven (+) and driver solution (−). It is worthy of mention that the Runge-Kutta integration uses the linear coordinate w along the solution trajectory as the independent variable similarly to [5], putting $dt/dw = 1 / \sqrt{1 + (dx/dt)^2 + (d\varepsilon_{//}/dt)^2 + (dz/dt)^2}$, $dx/dw = (dx/dt)(dt/dw)$, etc., and computing the derivatives with respect to t by division of Eqs. (3.16), (3.17) and (3.18) by Eq. (3.15), or else by means of Eqs. (4.1) and (4.2) at the orthogonal point.

The angular coordinate θ is then obtained by integration of Eq. (3.15), suitably modified to avoid the improper integration:

$$\theta \sqrt{\cos^2 \alpha - f^2 \sin^2 \alpha} = \pm \int_{t_o}^t \left[\frac{1}{\sqrt{(k_1 z - t)(t - k_2 z)}} - \frac{C}{\sqrt{\pm(t - t_o)}} \right] dt + 2C \sqrt{\pm(t - t_o)}$$

$$\text{where } C = \lim_{t \rightarrow t_o, z \rightarrow t/k_1} \sqrt{\frac{\pm(t - t_o)}{(k_1 z - t)(t - k_2 z)}} = \sqrt{\frac{\pm k_1 u_{\pm}}{\left(k_1 \frac{\tau_{C\perp}}{\tau_{R\perp}} - u_{\pm}\right)(k_1 - k_2)t_o}}$$

In this manner the function to be integrated does not diverge for $t \rightarrow t_o$, but tends to zero.

After reaching a sufficient convergence in the first phase of the minimisation process (10^{-4}), the starting elongation is varied as well according to the method described before.

Some constraints are imposed to the progressing solution. The width of each region is continuously controlled so that it does not become negative: if this occurs, the width is equated to zero. The largest elongation must be lower than the largest dimensionless tension t and the lowest elongation must be larger than the lowest value of t : if this condition is violated, $\epsilon_{//}$ is equated to t .

5. RESULTS

Figure 3 a shows the results for a drive where typical values of the viscous retardation times were imposed to the cord and rubber materials [11]. The influence of the belt viscoelasticity is insignificant in practice, as can be deduced by the nearly coincident diagrams of the forces and deformations.

On the contrary, Fig. 3 b shows a hypothetical case where the retardation times were "artificially" increased somehow. The increase of the viscoelastic resistance in the longitudinal direction, i. e. in the cord, gives rise to remarkable differences, particularly in the main sliding region. Since the wall elongation $\epsilon_w = B\epsilon_{//}$ gives a measure of the belt velocity and is nearly equal to the pulley peripheral velocity in the adhesion-like region, a lower difference between $\epsilon_{//adhesion-like}$ and $\epsilon_{//sliding}$, like in Fig. 3 b, indicates a reduction of the sliding velocity, which is to be considered as an advantage as regards the wear resistance of the belt. On the contrary, this result is scarcely useful as regards the efficiency, because it is somehow counterbalanced by the hysteresis losses during the load changes in the belt.

The increase of the longitudinal viscous properties of the belt can be obtained by a suitable choice of the cord material. As a pure example, some InSn alloys used for the manufacture of composite panels exhibit very large values of both the elastic modulus and the loss factor [11] and might be conveniently used to reinforce the belt and reduce the slip. Maybe, other important aspects should be taken into consideration, such as the production economy or the operative reliability, addressing towards other types of materials, but the present study just wants to point out the influence of viscoelasticity on the belt behaviour and the possible achievable benefits.

6. CONCLUSION

A thorough theoretical insight into the mechanics of viscoelastic V-belt drives is presented and some benefits achievable for what concerns the wear resistance are pointed out. The belt viscous response is also detected by quasi-static experiments.

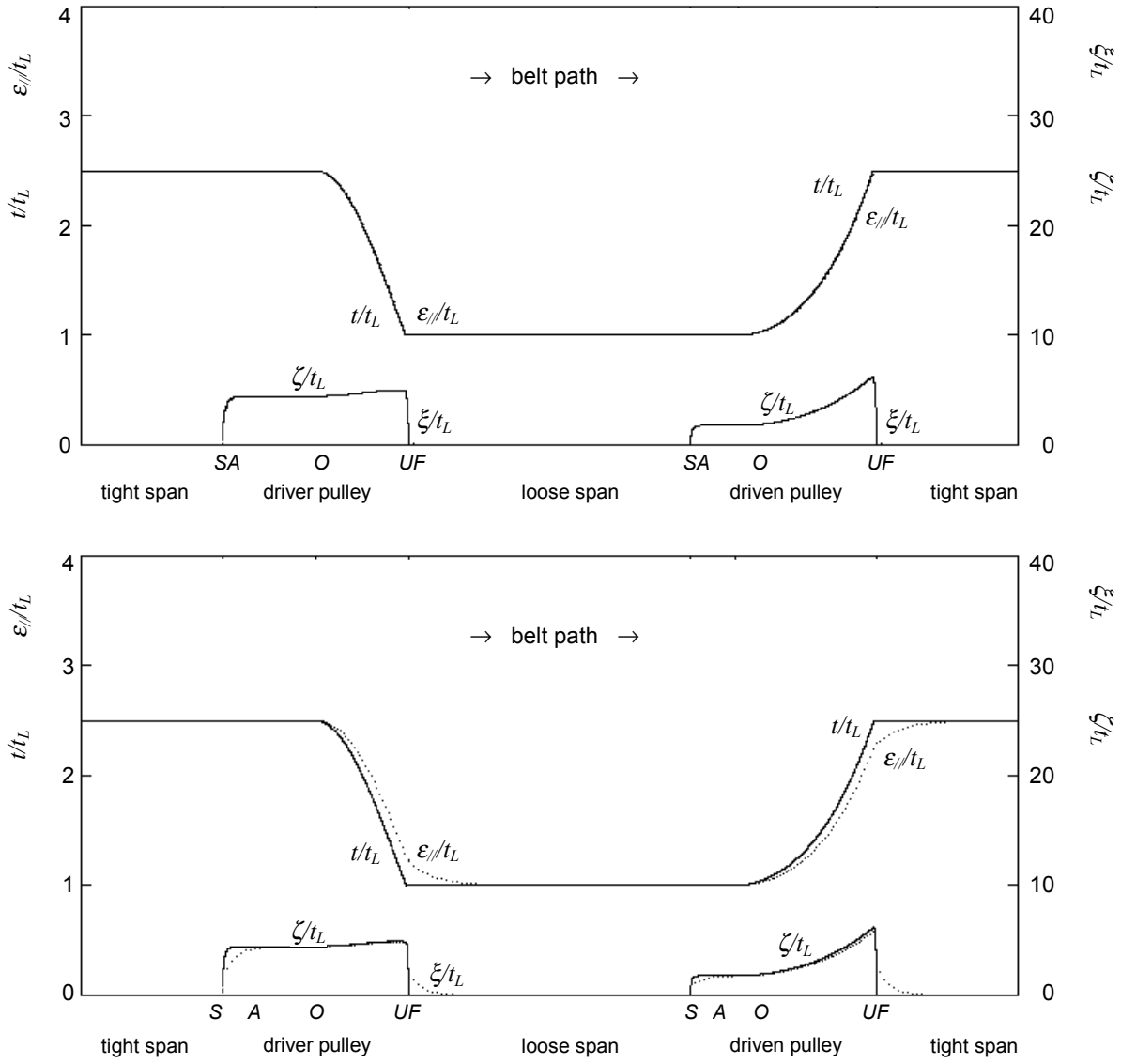


Figure 3. Longitudinal and transverse force and deformation

$$\xi = x r_0 / \bar{r}_0 = \varepsilon_{\perp} H / \bar{r}_0, \quad \zeta = z r_0 / \bar{r}_0, \quad \bar{r}_0 = (\text{belt half-length} - \text{centre-distance}) / \pi$$

(a): $\omega\tau_{R//} = .04, \omega\tau_{C//} = .06, \omega\tau_{R\perp} = .02, \omega\tau_{C\perp} = .03$. (b): $\omega\tau_{R//} = .2, \omega\tau_{C//} = .4, \omega\tau_{R\perp} = .1, \omega\tau_{C\perp} = .2$

Other data: $f = .3, \alpha = 14^\circ, k = .15, B = 2.5, T_T / T_L = 2.5, \omega_{driven} / \omega_{driver} = 1$

It is known that the viscous resistance of polymers can be modified to some degree, within certain limits, by a suitable manufacturing process. This opens interesting views in the technology of rubber belts and in their application fields.

ACKNOWLEDGEMENT

The authors thank the Italian Ministry M.I.U.R. for supporting this research financially.

REFERENCES

- [1] Sorge, F. and Cammalleri, M., "Viscoelastic Response of Rubber Belts", 15th Congress AIMETA, Taormina (ME), Italy, September 26-29, 2001.
- [2] Sorge, F., "Influence of Viscoelasticity on Rubber V-Belt Mechanics", AIMETA International Tribology Conference, Vietri sul Mare (SA), Italy, September 18-20, 2002.
- [3] Malvern L. E., "Introduction to the Mechanics of a Continuous Medium", Prentice-Hall, Englewood Cliffs (NJ), USA, 1969.
- [4] Sorge, F., Beccari, A. and Cammalleri, M., "Operative Variator Characterization for CVT Improvement", JSME Intern. Conference on Motion and Power Transmission, Fukuoka, Japan, November 15-17, 2001.
- [5] Sorge, F., "A Qualitative-Quantitative Approach to V-Belt Mechanics", ASME Journ. of Mech. Design, Vol. 118, n. 1, 1996.
- [6] Sorge, F., "Boundary V-Belt Mechanics", 14th Congress AIMETA, Como, Italy, October 6-9, 1999.
- [7] Gerbert, G., "Traction Belt Mechanics", Chalmers University of Technology, Göteborg, Sweden, 1999.
- [8] Gerbert, G. and Sorge, F., "Full Sliding "Adhesive-Like" Contact of V-Belts", ASME, DETC2000/PTG Conference, Baltimore (MA), USA, September 10-13, 2000.
- [9] McGhee, R. B., "Some Parameter Optimization Techniques", Digital Computer User's Handbook, Chapt. 4.8, M. Klerer and G. A. Korn Ed., McGraw-Hill B. C., New York, USA, 1967.
- [10] Lutz, O., "Zur Theorie des Keilscheiben-Umschlingungsgetriebe", Konstruktion, 12, 1960.
- [11] Brodt, M. and Lakes, R. S., "Composite Materials Which Exhibit High Stiffness and High Viscoelastic Damping", J. Composite Materials, 29, 1995.